IEEE Access
Multidisciplinary : Rapid Review : Open Access Journal

Received June 1, 2021, accepted June 11, 2021, date of publication June 17, 2021, date of current version June 28, 2021.

Digital Object Identifier 10.1109/ACCESS.2021.3090089

Exploiting the Inherent Flexibility in Transmission Network for Optimal Scheduling, Wind Power Utilization, and Network Congestion Management

MUHAMMAD NUMAN, AKIF ZIA KHAN, MANSOOR ASIF, SARMAD MAJEED MALIK, AND KASHIF IMRAN
Department of Electrical Engineering, National University of Sciences and Technology (NUST), Islamabad 44000, Pakistan
Corresponding author: Muhammad Numan (numan@uspcase.nust.edu.pk)

This work was supported by the US-Pakistan Center of Advanced Studies in Energy (USPCAS-E), National University of Science and Technology (NUST), Islamabad, Pakistan.

ABSTRACT Owing to the economic, social, and political problems in the expansion of transmission infrastructure, novel transmission topologies are in demand to efficiently utilize the existing infrastructure. On the other hand, there is a tremendous increase in wind power generation around the globe. One of the main challenges hindering the penetration of large-scale wind power generation is the network congestion due to limited network capacity. To address these two issues, this study develops a co-optimized optimal transmission switching (OTS) and dynamic line rating (DLR) model to optimize system resources by mitigating network congestion and maximizing wind power accommodation. This new concept of exploiting the inherent flexibility in transmission network is named as flexible transmission dynamic line rating (FTDLR), which deploys OTS in coordination with DLR as a control tool to utilize existing assets. A two-stage stochastic unit commitment framework is used to deploy the proposed FTDLR model, which is used to dynamically increase the line capacity based on the meteorological parameters and at the same time optimally select candidate lines to be switched off from the network. A comprehensive analysis is performed to characterize the FTDLR performance on system operation cost, network congestion, and wind power curtailment. The proposed FTDLR model is further tested as a part of contingency analysis where both generator failure and transmission line outages are considered. Test results performed on the IEEE 24-bus network demonstrate that by using FTDLR, the service operator could substantially reduce system dispatch cost, improve wind power accommodation, and relieve network congestion. The scalability and feasibility of the FTDLR optimization problem is validated on the larger network of the IEEE 118-bus system.

INDEX TERMS Contingency analysis, dynamic line rating, network congestion, optimal transmission switching, renewable energy sources.

NOMENCLATURE

A. SETS

N	All buses indexed by i,j
S	All scenarios indexed by Ω
G	All generating units indexed by g
W	All wind farms indexed by w

B. PARAMETERS

T_{ij}, D	Conductor Temperature and diameter
q_{ij}^{l}, q_{ij}^{s}	Joule and Solar heat gain terms
q_{ij}^{c}, q_{ij}^{r}	Convection and Radiation heat loss
$q_{ij}^{c,n}, q_{ij}^{f,n}$	Natural and Forced convection
$R(T_{ij})$	Resistance of the conductor
LIR_{ij}	Line improvement rate for line ij
C_g^{NL}, C_g^{SU}	No-Load and Start-up cost of unit g
C_g^{V}	Production cost of unit g
$VOLL, C^{WC}$	Value of lost load and wind curtailment cost
P_g^{min}, P_g^{max}	Capacity limits of unit g
R_g^{up}, R_g^{dn}	Ramp up and Ramp down rate of unit g
P_g^{SU}, P_g^{SD}	Maximum output by unit g during start-up and shut-down
SR_g^{max}	Maximum spinning reserves
SR_g^{min}	Minimum spinning reserves
$SR_{g,t}$	Spinning reserves at time t
$SR_t^{reqd\_min}$	Required minimum spinning reserves during time t
$RR_{g,t}$	Ramp rate of generator g

The associate editor coordinating the review of this manuscript and approving it for publication was R. K. Saket.

t_g^{up}, t_g^{dn}	Minimum time for unit g to On/Off
$P_{w,t,\Omega}$	Power output of wind farm w
$D_{i,t}$	Bus i demand at time period t
x_{ij}, B_{ij}	Line ij Reactance and Susceptance
π_Ω	Probability of scenario Ω.
$f_{ij}^{max,SLR}, f_{ij}^{max,DLR}$	Maximum SLR and DLR rating for line ij
δ_{ij}^{max}	Maximum bus voltage angle difference
z_{max}^{off}	Limit on lines switching actions
z_{max}^{DLR}	Maximum number of lines adopting DLR ratings
$h_{g,t,\Omega}, h_{ij,t,\Omega}$	Index for healthy/contingency state of generator and transmission line

C. VARIABLES

$u_{g,t,\Omega}$	On/Off Status binary variable of generator
$y_{g,t,\Omega}$	Start-up indicator for unit g
$P_{g,t,\Omega}$	Unit g output power
$f_{ij,t,\Omega}^{s}, f_{ij,t,\Omega}^{ns}$	Power flow through switchable and non-switchable lines
$\delta_{i,t,\Omega}$	Voltage angle of bus at node i
$z_{ij,t,\Omega}^{off}$	Variable indicating switching status of line ij
$z_{ij,t,\Omega}^{SLR}$	Variable indicating line ij in SLR state
$z_{ij,t,\Omega}^{DLR}$	Variable indicating line ij in DLR state
$L_{i,t,\Omega}, L_{i,t,\Omega}^{w}$	Load-shedding and wind curtailment
$SR_{g,t}^{schd}$	Scheduled spinning reserves
$SR_{g,t,\Omega}^{deply}$	Deployed spinning reserves

I. INTRODUCTION

A. LITERATURE REVIEW

Recently, wind power generation is increasing at a rapid rate due to its free carbon emission source and lower production cost. Although the penetration of large-scale wind power resources is accompanied by several benefits, the output of wind power is characterized by uncertainty and variability. This immense integration of wind resources into the network poses numerous challenges for the economic and secure operation of the system because of the uncertain nature of wind. The main challenge is the stable operation of power networks at times of high levels of wind power output. With the increased penetration of wind resources, a substantial volume of wind power is curtailed in practice [1]. The increasing penetration of renewable generation also leads to network congestion, which further increases cost of generation and restrict the large scale integration of renewable energy resources [2]. One solution to mitigate system congestion and facilitate integration of wind resources is to build new transmission lines but building new infrastructure is quite expensive and time consuming, which will undermine the social and economic benefits achieved from the implementation of wind power generation. Therefore, there is a greater demand for new topologies to efficiently exploit the existing assets without building new infrastructure.

Network congestion is mainly caused due to insufficient transmission line capacity to deliver power from the area of generation to load centers. System congestion obstructs effective utilization of wind power as the surplus wind power production has to be curtailed, which leads to revenue uncertainty for wind power producers. The uncertain and variable nature of wind energy resources makes it even more challenging to maximize its utilization in congested networks. The impact of network congestion is more drastic under contingency. When an element in the network fails, the remaining elements in the network may experience more loading, which can further exacerbate the risk of network congestion. Therefore, even a system may have no congestion with efficient utilization of wind power, there is high probability that any outage in the network will severely change the situation.

The high penetration of wind power generation needs more flexible resources, which can help to mitigate the uncertainties from these kinds of resources and alleviate network congestion [3]. One way to achieve system flexibility is to deploy Optimal Transmission Switching (OTS) action. OTS is a technique where the status of the lines is treated as a variable rather than a fixed parameter [4]. In literature, OTS is shown to provide economic benefits by reducing system dispatch cost [5]–[7], relieve voltage violations [8], and improve renewable generation integration [9]–[14]. Furthermore, it is shown that OTS can help in load-shedding recovery [15] and reduce the cost associated with network expansion planning [16],[17]. OTS in coordination with unit commitment can provide operators the option to alter network topology [18]. Reliability of power system is of prime importance and it must be ensured that the switching actions of OTS does not compromise system reliability. This issue is studied in detail by different authors in [18]–[23] and it is concluded that the system reliability can still be maintained with OTS enforcement in both stochastic and deterministic modeling. Another main advantage of OTS enforcement is that it can help relieve network congestion significantly [24], [25]. It is demonstrated that system congestion mitigation can be achieved by deploying OTS, which exploits the inherent flexibility in transmission assets to enhance power system operation. The implementation of OTS is limited by factors such as computational complexity and concerns about system stability. The incorporation of OTS with battery energy storage systems is also studied by different authors and it is showed that transmission topology using network reconfiguration can efficiently use battery energy storage systems for optimal system performance [26]–[28].

Recently, different heuristics and algorithms are developed to assess the computational complexity of problems with OTS [29]–[33]. These results show that OTS problem for large-scale power system can still be solved within a realistic amount of time. A major development in the implementation of OTS in real power system networks is addressed in [34] where the authors proposed a real-time contingency analysis incorporating transmission switching acting as a corrective mechanism. With the advent of smart grid technologies, soon

OTS approach can be implemented in real networks and make a great impact in multi-million dollar power industry.

Conventionally, worst case weather scenarios are used to rate transmission lines, which is termed as static line rating (SLR). Weather conditions, however, are not constant in actual and changes continuously. This means that the actual rating of a transmission line could be underestimated using the SLR ratings. Meanwhile, using dynamic line rating (DLR) the service operator can determine the actual line ampacity in real time [35]–[37]. In literature DLR is used to increase the rating of the transmission line in real time, which helps improve renewable integration, mitigate network congestion, and enhance power system reliability [38]. DLR is also used in transmission expansion problems. It is shown that using DLR in the existing network can help delay the need for installing new transmission lines [39]. It is also shown that system security can still be preserved while enforcing DLR in a security constrained UC problem [40]. DLR is applied in a stochastic security constrained UC formulation to capture wind power uncertainty [41]. The author in [42] used pre-specified DLR values in conjunction with network reconfiguration to reduce the uncertainty linked with renewable generation. The deployment of the DLR is also cheap as compared to installing new transmission lines. It is shown that the cost associated with deploying DLR is no more than 2% of the cost needed to obtain the same advantage by installing new transmission lines [43], [44]. With advancement in technology, it is now possible to use DLR in a day-ahead power system scheduling problem to gain more optimized and economical scheduling [37], [45].

B. RELATED WORK

These two smart grid technologies (OTS and DLR) possess some shared features i.e. they both can help reduce network cost and enhance power system ability to transfer more power through lines, which helps in postponing the installation of new transmission lines. The coordination of OTS and DLR with other technologies is recently studied only by few authors. In [46] OTS and DLR along with bus-splitting mechanism is incorporated in a day-ahead scheduling process for improved integration of renewable generation resources. The authors in [47] presented a network-constrained direct current optimal power flow problem by jointly enforcing OTS and DLR. The reliability of the joint operation of OTS and DLR is assessed in [48], where the authors showed that instead of degrading system reliability, the combined OTS and DLR topology can improve system reliability. Investment planning and transmission expansion problem using reconfigurable networks and DLR are studied in [49], [39], [50].

C. RESEARCH GAP

However, the current literature about the DLR enforcement with OTS in scheduling of power system network is based on deterministic modeling. Considering the variable and uncertain nature of wind power, it is necessary to consider this uncertainty in the UC problem. In contrast to deterministic modeling, stochastic optimization is widely used as a powerful tool for problems involving uncertainties. In this paper, we fill the gap in the current literature to mobilize transmission system inherent flexibility by simultaneously deploying OTS and DLR in a security-constrained SUC formulation to consider the wind power uncertainty.

D. RESEARCH CONTRIBUTION

The major contributions of this paper are:

1. To simultaneously deploy OTS and DLR in a security constrained SUC problem for optimal, secure, and reliable power system operation. The co-optimization of DLR and OTS for improved wind power integration in a security constrained UC formulations is not discussed in the current literature.
2. The proposed model is used to identify optimal transmission lines, which produce optimal performance when switched off from the network. At the same time the optimization problem is used to determine suitable lines for adopting DLR based on the meteorological conditions.
3. To quantify the efficacy of the optimization problem, a comprehensive analysis is performed including dispatch cost, wind power curtailment, and congestion management analysis.
4. The proposed FTDLR model is further tested as a part of contingency analysis where both generator failure and transmission line outages are considered in the test cases to show that the FTDLR model still maintains the security of the system.

The remaining of the paper is presented as follows: Model formulation and objective function along with constraints is explained in section II. Solution methodology and case study simulations on IEEE 24-bus and 118-bus systems are performed in section III to demonstrate the performance of the proposed model. This section also includes analysis of the model on system cost, wind power curtailment, network congestion, and contingency analysis. The paper is concluded in section IV with future research directions.

II. MODEL FORMULATION

Following [51], the optimization problem is molded as a two-stage SUC problem, where generating units are partitioned into slow-units and fast-units depending on their commitment in the two-stage decision process. Based on the predicted load and weather parameters, first-stage decisions consist of the status of the slow-units. Subsequently, as the uncertainty of wind power is revealed, fast-units commitments and the generation of all units are all carried out in the second-stage of the model.

The proposed two-stage decision problem modeled in a SUC framework. Decision variables in the model are divided into two groups: First-stage and Second-stage decisions. Network information is collected in the pre-processing step and analyzed along with the network topology. This information is then passed to the UC stage. In this stage, the optimization problem determines the commitment of generating units, which are to be turned on/off, as well as the contribution of the spinning reserves of each unit. The network information in this stage is limited and only takes into account critical transmission elements. A sufficient number of units should be committed to surpass the expected load plus the requirement of the spinning reserves. First-stage decisions represents day-ahead decisions and are equally exercised for all the realized scenarios. Decisions in the second-stage are here and now response actions to the realized uncertainty. Second-stage variables include dispatch of generators, spinning reserves deployment, and status of the transmission lines. In case, the reserves scheduled in the first-stage are insufficient to meet the demand, it results in supply inadequacy and may result in an increase in load-shedding. A signal is generated for the first-stage decisions so that appropriate reserves can be procured. This stage also evaluates the contingency analysis and determines the base case power flow solution in terms of N-1 requirements. To reduce the computational complexity, only critical contingencies are considered in the stochastic economic dispatch (SED) step. The obtained solution from the SED stage is passed to operator review stage, where it is reviewed by Service Operator (SO) and necessary changes are made depending on the constraint violations and solution quality. If a solution is not acceptable, the problem is solved again unless an acceptable solution is obtained.

The ratings of a transmission line is determined through technical standards presented by different international organizations. The most important of these are the CIGRE Brochure 601 [52], IEEE standard 738 [53], and IEC/TR 61597 standards [54]. The heat balance equation (HBE) for steady-state condition in the IEEE 738 standard is used in this paper and given by (1).

$$q_{ij}^{l}+q_{ij}^{s}-q_{ij}^{c}-q_{ij}^{r}=0 \tag{1}$$

Joule heating (q_{ij}^{l}) and solar radiations (q_{ij}^{s}) heats the conductor while convection (q_{ij}^{c}) and radiation (q_{ij}^{r}) heat losses cools the conductor. The current through a conductor can then be determined using (2) by rearranging the terms in (1).

$$I_{ij}=\sqrt{\frac{1}{R\left(T_{ij}\right)}\left(q_{ij}^{c}+q_{ij}^{r}-q_{ij}^{s}\right)} \tag{2}$$

Based on the anticipated weather conditions, the dynamic capacity of the transmission lines using DLR is calculated. To compare the rating values obtained from SLR and DLR, line improvement rate (3) is used, which shows the improvement in line when DLR is deployed as compared to SLR. The line ratings to be used in the optimization problem are then updated using (4) [48].

$$LIR_{ij}=\frac{I_{\max,DLR}-I_{\max,SLR}}{I_{\max,SLR}} \tag{3}$$

$$f_{ij}^{DLR}=\left(1+LIR_{ij}\right)f_{ij}^{SLR} \tag{4}$$

The proposed formulation of the coordinated operation of FTDLR in a two-stage SUC formulation can be presented by the objective function in (5) and the constraints in (6)-(38). The constraints of the FTDLR model are divided into first-stage and second-stage constraints.

A. OBJECTIVE FUNCTION

$$\min\left\{\begin{array}{l}\sum_{g\in G_1}\sum_{t\in T}\left(C_g^{NL}u_{g,t}+C_g^{SU}y_{g,t}\right)+\\ \sum_{\Omega\in S}\sum_{t\in T}\pi_\Omega\left\{\begin{array}{l}\sum_{g\in G_2}(C_g^{SU}y_{g,t,\Omega}+C_g^{V}P_{g,t,\Omega})\\ +\sum_{w\in W}C^{WC}P_{w,t,\Omega}^{WC}+\\ \sum_{i\in N}L_{i,t,\Omega}\,VOLL_{i,t}\end{array}\right\}\end{array}\right\} \tag{5}$$

The main objective is to minimize the total system operating cost, which includes the cost of generation, penalty cost for load-shedding, and wind curtailment cost. Generating unit start-up cost C_g^{SU} depends on the unit commitment states $u_{g,t}$ and is irrelevant of the probability of the scenario π_Ω. On the contrary, production cost of generators C_g^{V}, penalty cost for load-shedding $VOLL_{i,t}$, and wind curtailment cost C^{WC} are calculated after the realization of the uncertainty.

B. FIRST-STAGE CONSTRAINTS

$$\sum_{g\in G}P_{g,t}+\sum_{w\in W}P_{w,t}+\sum_{j\in k(i)}f_{ij,t}-\sum_{q\in k(i)}f_{qi,t}=D_{i,t} \quad (\forall i,t) \tag{6}$$

$$P_g^{\min}u_{g,t}\le P_{g,t}\le P_g^{\max}u_{g,t}\;\forall t,g\in G_1 \tag{7}$$

$$-f_{ij,t}^{\max}\le f_{ij,t}\le f_{ij,t}^{\max}\;\forall ij,t \tag{8}$$

$$y_{g,t}=u_{g,t}-u_{g,t-1}\forall t,g\in G_1 \tag{9}$$

$$0\le SR_{g,t}^{schd\_up}\le P_g^{\max}-P_{g,t}\;\forall g,t \tag{10}$$

$$SR_{g,t}^{schd\_up}\le SR_g^{\max}u_{g,t}\;\forall g,t \tag{11}$$

$$0\le SR_{g,t}^{schd\_dn}\le P_{g,t}-P_g^{\min}\;\forall g,t \tag{12}$$

$$SR_{g,t}^{schd\_dn}\ge SR_g^{\min}u_{g,t}\;\forall g,t \tag{13}$$

$$\sum_g SR_{g,t}\le SR_t^{reqd\_\min}\;\forall g,t \tag{14}$$

$$\left|P_{g,t}-P_{g,t-1}\right|\le RR_g\;\forall t,g\in G_1 \tag{15}$$

$$\sum_{t=\tau}^{t_g^{up}-1+\tau}u_{g,t}\ge\left(-u_{g,\tau-1}+u_{g,\tau}\right)t_g^{up}\quad \forall t,g\in G_1\,(2\le\tau\le 1+T-t_g^{dn}) \tag{16}$$

$$\sum_{t=\tau}^{t_g^{dn}-1+\tau}\left(1-u_{g,t}\right)\ge\left(-u_{g,\tau}+u_{g,\tau-1}\right)t_g^{dn}\quad \forall t,g\in G_1\,(2\le\tau\le 1+T-t_g^{dn}) \tag{17}$$

Constraint (6) is the power balance constraint. Conventional generators are operated within their limits by (7). Power flow is restricted in lines by (8). Generator variables for start-up and unit commitment variables are linked by (9). Spinning reserve inequalities are imposed in (10)-(14). Ramp up/down rate of generators is imposed in constraint (15) while the minimum On/off time limits are satisfied in constraints (16) and (17) respectively.

C. SECOND-STAGE CONSTRAINTS

$$\sum_{g\in G} \hbar_{g,t,\Omega} P_{g,t,\Omega} + \sum_{w\in W} \hbar_{w,t,\Omega} P_{w,t,\Omega} + \sum_{ij\in N} \hbar_{ij,t,\Omega} \left(f^{s}_{ij,t,\Omega} + f^{ns}_{ij,t,\Omega}\right) + L_{i,t,\Omega} - D^{real}_{i,t,\Omega} = 0, \quad (\forall ij, g, t, \Omega) \tag{18}$$

The second-stage of the problem includes constraints for all the realized scenarios. The energy balance constraint in (18) is analogues to (6), and the indices $\hbar_{g,t,\Omega}$, $\hbar_{w,t,\Omega}$, and $\hbar_{ij,t,\Omega}$ indicate the healthy state of the generator, wind turbine, and transmission line respectively. If a facility cannot provide power due to maintenance or contingency, the corresponding index is set to zero to restrict the active power output.

$$z^{off}_{ij,t,\Omega} + z^{SLR}_{ij,t,\Omega} + z^{DLR}_{ij,t,\Omega} = 1, \forall ij, t, \Omega \tag{19}$$

The line status in FTDLR is presented by binary variables $z^{off}_{ij,t,\Omega}$, $z^{SLR}_{ij,t,\Omega}$, and $z^{DLR}_{ij,t,\Omega}$. Line ij is off if $z^{off}_{ij,t,\Omega}$ =1 during time t in scenario Ω. SLR ratings are used when $z^{SLR}_{ij,t,\Omega}$ =1. At times of the favorable windy weather conditions when the real-time line rating is greater than the SLR, the optimization problem sets $z^{DLR}_{ij,t,\Omega}$ =1. Constraint (19) is used to make sure that the line remains in only one state at each time period.

$$f^{s}_{ij,t,\Omega} \geq -\hbar_{ij,t,\Omega} \left(f^{\max,SLR}_{ij} z^{SLR}_{ij,t,\Omega} + f^{\max,SLR}_{ij} \left(1 + LIR_{ij,t,\Omega}\right) z^{DLR}_{ij,t,\Omega} \right) \quad (\forall ij, t, \Omega) \tag{20}$$

$$f^{s}_{ij,t,\Omega} \leq \hbar_{ij,t,\Omega} \left(f^{\max,SLR}_{ij} z^{SLR}_{ij,t,\Omega} + f^{\max,SLR}_{ij} \left(1 + LIR_{ij,t,\Omega}\right) z^{DLR}_{ij,t,\Omega} \right) \quad (\forall ij, t, \Omega) \tag{21}$$

$$f^{s}_{ij,t,\Omega} - \left(\delta_{i,t,\Omega} - \delta_{j,t,\Omega}\right) \big/ x_{ij} + M_{ij,t,\Omega} z^{off}_{ij,t,\Omega} \geq 0 \quad (\forall ij, t, \Omega) \tag{22}$$

$$f^{s}_{ij,t,\Omega} - \left(\delta_{i,t,\Omega} - \delta_{j,t,\Omega}\right) \big/ x_{ij} - M_{ij,t,\Omega} z^{off}_{ij,t,\Omega} \leq 0 \quad (\forall ij, t, \Omega) \tag{23}$$

$$-\hbar_{ij,t,\Omega} f^{\max}_{ij,t,\Omega} \leq f^{ns}_{ij,t,\Omega} \leq \hbar_{ij,t,\Omega} f^{\max}_{ij,t,\Omega} \forall ij, t, \Omega \tag{24}$$

$$f^{ns}_{ij,t,\Omega} = \hbar_{ij,t,\Omega} \left(\delta_{i,t,\Omega} - \delta_{j,t,\Omega}\right) / x_{ij} \forall ij, t, \Omega \tag{25}$$

Transmission lines in the network are classified into switchable lines and non-switchable lines. Constraints (20)-(23) restricts the flow limit on switchable lines. Power flow through a line is zero when $z^{off}_{ij,t,\Omega}$ =1. Otherwise, the line will remain in service and the flow in it will not exceed its limits. Kirchhoff's current law in a modified form is used in (22) and (23) to make sure when a line is removed from the system, the flow through the line is zero regardless of the voltage angle between the buses. The value of the big M is estimated to be equal or greater than $B_{ij}\left(\delta^{\max}_{i} - \delta^{\max}_{j}\right)$. The flow of power through non-switchable lines is limited by (24) and (25).

$$P_{g,t,\Omega} = \hbar_{g,t,\Omega} \left(P_{g,t} + SR^{deploy\_up}_{g,t,\Omega} - SR^{deploy\_dn}_{g,t,\Omega}\right) \quad (\forall g, t, \Omega) \tag{26}$$

$$0 \leq SR^{deploy\_up}_{g,t,\Omega} \leq SR^{schd\_up}_{g,t,\Omega} \hbar_{g,t,\Omega} \forall g, t, \Omega \tag{27}$$

$$0 \leq SR^{deploy\_dn}_{g,t,\Omega} \leq SR^{schd\_dn}_{g,t,\Omega} \hbar_{g,t,\Omega} \forall g, t, \Omega \tag{28}$$

The power generation schedule is adjusted using the reserve variables in each scenario, as given in (26). The constraints in (27) and (28) link the scheduled spinning reserves in the first-stage to that deployed in the second-stage. The reserves scheduled in the first-stage should be sufficient enough to prevent load-shedding. Spinning reserves can be only delivered by the units in healthy state i.e. $\hbar_{g,t,\Omega} = 1$.

$$P_{g,t,\Omega} - P_{g,t-1,\Omega} \leq \left(2 - u_{g,t-1,\Omega} - u_{g,t,\Omega}\right) P^{SU}_{g} + \left(1 + u_{g,t-1,\Omega} - u_{g,t,\Omega}\right) R^{up}_{g} \ \forall g, t, \Omega \tag{29}$$

$$P_{g,t-1,\Omega} - P_{g,t,\Omega} \leq \left(2 - u_{g,t-1,\Omega} - u_{g,t,\Omega}\right) P^{SD}_{g} + \left(1 - u_{g,t-1,\Omega} + u_{g,t,\Omega}\right) R^{dn}_{g} \ \forall g, t, \Omega \tag{30}$$

$$\sum_{t=\tau}^{t^{up}_{g}-1+\tau} u_{g,t,\Omega} \geq \left(-u_{g,\tau-1,\Omega} + u_{g,\tau,\Omega}\right) t^{up}_{g} \quad \forall g, t, \Omega (2 \leq \tau \leq 1 + T - t^{up}_{g}) \tag{31}$$

$$\sum_{t=\tau}^{t^{dn}_{g}-1+\tau} \left(1 - u_{g,t,\Omega}\right) \geq \left(-u_{g,\tau,\Omega} + u_{g,\tau-1,\Omega}\right) t^{dn}_{g} \quad \forall g, t, \Omega (2 \leq \tau \leq 1 + T - t^{dn}_{g}) \tag{32}$$

$$0 \leq P^{WC}_{w,t,\Omega} \leq P_{w,t,\Omega} \forall w, t, \Omega \tag{33}$$

Generators ramping requirement for each scenario is enforced in (29) and (30), while the minimum up/down time constraints in each scenario are represented in (31) and (32) respectively. The amount of wind power curtailment is restricted by (33).

$$\sum_{ij\in N} z^{off}_{ij,t,\Omega} \leq z^{off}_{\max}, \forall ij, t, \Omega \tag{34}$$

$$\sum_{ij\in N} z^{high}_{ij,t,\Omega} \leq z^{high}_{\max}, \forall ij, t, \Omega \tag{35}$$

$$\sum_{ij\in N_i} \left(1 - z^{off}_{ij,t,\Omega}\right) \geq 1, \forall ij, t, \Omega \tag{36}$$

$$z^{off}_{ij,t,\Omega}, z^{norm}_{ij,t,\Omega}, z^{high}_{ij,t,\Omega} \in \{0, 1\} \tag{37}$$

$$u_{g,t,\Omega}, y_{g,t,\Omega} \in \{0, 1\} \tag{38}$$

Constraints (34) and (35) are used to limit the maximum number of lines for switching operation and lines adopting DLR values. Constraint (36) is used to prevent islanding the network when some lines are switched off. Binary variables in (37) and (38) are used to represent status of the lines as well as the generating units on/off and start-up.

III. CASE STUDY SIMULATIONS

Two case studies on IEEE 24-bus and 118-bus systems are performed to validate the performance of the FTDLR model. Due to computational complexity, only the uncertainty associated with wind speed is used in this paper as a prominent factor for determining DLR values. A large number of scenarios are required to accurately represent the uncertainty associated with wind power production. We used Monte Carlo simulations to generate thousands of scenarios. These scenarios are then reduced to few representative scenarios using the scenario reduction technique. A 24h horizon period is set for the scheduling problem. It is assumed that the failed components cannot be replaced or repaired, as the operation time considered is relatively shorter than the time required for maintenance or repairing. To focus on the synergetic effect of the FTDLR model in the presence of contingencies, multiple outages or sequential component failure is not considered in this study.

The proposed FTDLR model is a mixed integer linear programming (MILP) problem. CPLEX, a commercial solver is used to solve the model. To speedup solution time of the optimization problem, we provide a warm-start solution to the main problem using the built-in function (addMIPStart) of the CPLEX. This function helps CPLEX in finding the initial solution to the problem and then passing it to the main problem. Firstly, a SUC problem is solved without transmission switching to get the commitment decisions for the generating units in the first-stage. These decisions are then fed as warm-start values for the main optimization problem through a flow-control script. Secondly, a DC-OPF problem is solved using OTS to find candidate transmission lines that can improve system performance when switched off from the network. From previous research [55], it is observed that we only need a small fraction of the total number of lines for switching actions to get optimal performance while still maintaining system security. The selection of candidate lines for switching actions is determined using [23] by classifying transmission lines as switchable and non-switchable lines. Candidate lines for switching actions are those lines which can reduce system operating cost and if these are removed from the network, they have very little or no effect on the cost of load not served. On the other hand, transmission lines categorized as non-switchable lines are those line, which if switched off from the network, severely effect system security as well as increase the system cost. The process of line categorization is explained in our previous article [56].

IBM ILOG CPLEX Optimization Studio OPL language is used for modeling the optimization problem. The solver used in CPLEX version 12.7.1. An Intel equipped core i7 CPU Desktop PC is used for running the optimization problem having 24GB of installed RAM

A. IEEE 24-BUS SYSTEM

The IEEE 24-bus system consists of 24 buses with 34 transmission lines and 10 load busses. The maximum generation capacity of the system is 3375MW while maximum load is 2950MW. System parameters and cost information is obtained from [57]. Following [36], the ratings of some transmission lines are modified to make the system more congested and better assess the impact of the co-optimized formulation on system performance. The line ratings of the lines 25, 26, and 27 are reduced to 175MW while for line 21 it is assumed to be 220MW. All other lines ampacities are decreased by 0.9p.u of the original ratings. The maximum increase in DLR values is set as 20% to guarantee secure power system operation. All overhead transmission lines are assumed to be standard 26/7 ACSR conductors. To calculate the thermal ratings, IEEE standard 738 [53] is used. In general all lines can be considered to adopt DLR values, but in this paper to better assess the performance of the proposed FTDLR model only lines connected with the buses with farms are considered. Two wind farms have rated power of 350MW and 450MW are used at Bus-3 and Bus-24 respectively. The cost of wind spillage is assumed to be 60$/MWh and the cost of load shedding as penalty is set to 1000$/MWh.

The performance of the two-stage decision model using stochastic programming depends heavily on the set of generated scenarios that are put into the problem and their relative weight with respect to each other. The main challenge is to select a fewer number of scenarios that are representative and can guide the SUC program to devise a UC schedule that can reduce system costs as compared to a deterministic UC schedule. Following [58], Monte Carlo simulations is used for random scenario generation. Thousand scenarios are generated to take into account wind power uncertainty [59]. However, as the main focus of this research is to assess the operational performance of the co-optimized model over the basic SUC formulation, a reduced set of scenarios presented in Figure 1 is used to represent wind power output uncertainty and will be used in the rest of the test cases results.

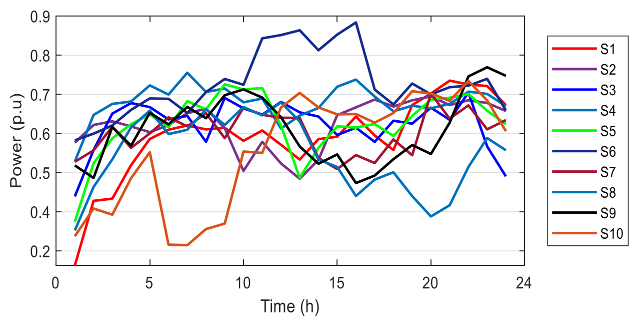

FIGURE 1. Reduced set of representative wind power output scenarios.

In order to comprehensively study the efficacy of the FTDLR model, four test cased are studied, including a) SUC, b) OTS, c) DLR and d) FTDLR with both OTS and DLR enforced. FTDLR model topology for the IEEE 24-bus system is shown as nodal representation in Figure 2.

1) DISPATCH COST ANALYSIS

System dispatch costs for the above-mentioned four cases is summarized in Table 1. There is no line switching operation

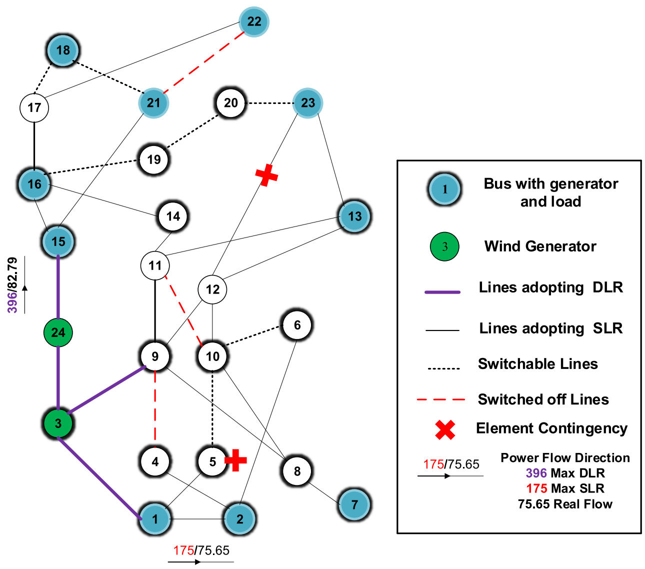

FIGURE 2. Nodal representation of the FTDLR model for IEEE 24-bus system.

TABLE 1. Dispatch cost results for the IEEE 24-bus system.

Method	Operating Cost (M$)				Cost Saving (%)
	z=0	z=1	z=2	z=3	
SUC	0.534	-	-	-	N/A
DLR	0.491	-	-	-	8.05
OTS	-	0.458	0.457	0.452	15.35
FTDLR	-	0.416	0.415	0.420	22.28

in the basic SUC and DLR topologies. For OTS and FTDLR, different number of lines are permitted to be switched and the best solution found in the specified time is noted to further assess the effect of line switching operation on system operating cost. Although the prime objective is optimality, yet in a practical system, improving solution is more important than proving optimality. The main goal is to find the best solution for the optimization problem within the available time period. Savings in cost for the FTDLR model as compared to SUC, DLR, and OTS are 22.28%, 15.35%, and 8.05% respectively.

The hourly system operating cost for all the four test cases is displayed in Figure 3. Almost in all scenarios, FTDLR results in less operating cost in comparison to other topologies. The enforcement of DLR alone also produces less cost than the base case. In case of OTS, the system cost in hours 10 and 22 is more than that of SUC, DLR, and FTDLR. But the coordinated operation of OTS and DLR leads to the most economic system dispatch cost.

Cost comparison of generating units in the first-stage and second-stage units is compared in Figure 4. For better comprehension, the cost values are scaled through dividing the cost of each topology by the corresponding cost of SUC. The results displayed in Figure 4 depict that including FTDLR as

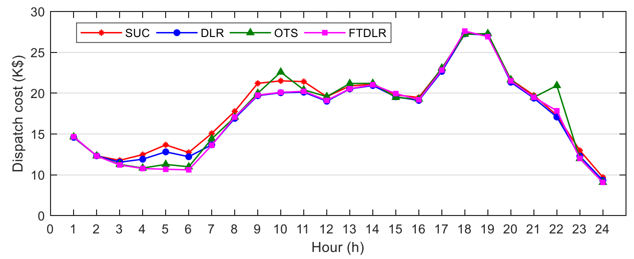

FIGURE 3. Hourly dispatch cost information for the four test cases.

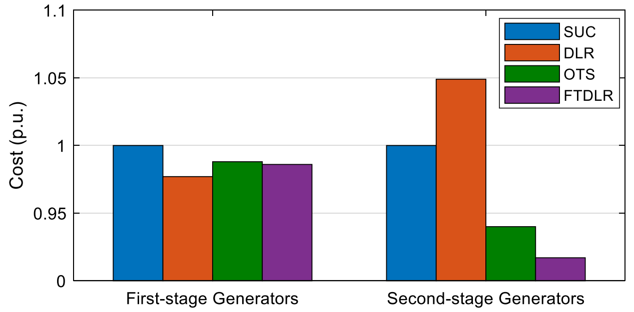

FIGURE 4. Cost comparison of first-stage and second-stage units for IEEE 24-bus System.

a recourse action, system dispatch decisions are changed so as to reduce the net operating cost. Almost the same amount of power is generated from first-stage units. The reduction in cost is mostly achieved by decreasing dispatch of generation from second-stage units. Around 9% less generation is dispatched by second-stage units in FTDLR. This reduction in the generation is covered by accommodating more wind power generation and from shifting the power from expensive units to cheaper ones in the first-stage units.

The line switching actions for OTS and FTDLR are compared in Table 2, which displays the status of the switchable lines for both OTS and FTDLR. The values (0/1) are inversed for line status for better understanding i.e. a 1 indicates line in service while 0 show the line is switched. Results indicate that the switching actions for both cases are not the same. It can be seen that the incorporation of FTDLR further reduces the number of switching actions as compared to OTS alone. This further validates the performance of FTDLR, which improves overall system performance with less number of switching actions.

The enforcement of FTDLR can help enhance wind power integration into the network in the presence limited transmission line capacity and network congestion. Sequential wind power curtailment information for the four test cases is presented in Figure 5.

It is noteworthy that wind power utilization level for FTDLR is highest in all the test cases. In basic SUC formulation, there is significant wind power curtailment due to potential network congestion and limited capacity to deliver wind power to other buses in the system. The wind curtailment savings for FTDLR as compared to SUC, DLR, and OTS are 96.84%, 93.23%, and 91.57% respectively.

TABLE 2. Status of switchable lines in OTS and FTDLR.

Lines	Method	1-6h	7-12h	13-18h	19-24h
4-9	OTS	110011	101110	111001	101100
	FTDLR	110111	111101	010111	111111
5-10	OTS	101101	011011	111111	111100
	FTDLR	111011	110111	111111	111110
6-10	OTS	111110	111111	110111	111011
	FTDLR	111111	110011	111001	101111
10-11	OTS	110001	111111	111111	011111
	FTDLR	101001	011111	111111	111111
16-19	OTS	111101	101111	111011	101111
	FTDLR	111101	111110	101101	111101
17-18	OTS	111111	111001	111111	110111
	FTDLR	111111	111111	111111	111111
19-20	OTS	101110	111111	111111	111111
	FTDLR	111111	111111	111111	111111
20-23	OTS	111111	111111	111111	111111
	FTDLR	111111	111111	111111	111111
21-22	OTS	111110	111111	111111	111111
	FTDLR	111111	111111	111111	111111

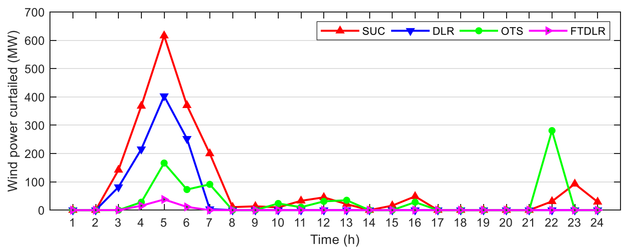

FIGURE 5. Hourly wind power curtailment for the IEEE 24-bus system.

2) CONGESTION MANAGEMENT ANALYSIS

To further understand the performance of the FTDLR, we examine the ramping capabilities, loading conditions, and congestion rate of the system. The congestion rate (CR) can be defined using the equation given in (39).

$$CR = \frac{\sum_{\Omega \in S} \pi_\Omega \sum_{t \in T} \sum_{ij \in N} 1.\left(\left|f_{ij,t,\Omega}\right| = f_{ij}^{\max}\right)}{(\#T)\,(\#N)} \tag{39}$$

CR is used to determine how a network is congested on average. Information of the generation and loading for the IEEE 24-bus system are shown in Table 3. The CR for OTS is used for $z_{\max}^{off}$ =3, while for FTDLR it is taken for $z_{\max}^{off}$ =2 where the optimization problem results in minimum dispatch cost. Network congestion information for all the test cases is given in Table 4.

The CR for the basic SUC is 6.87% while it reduces to 6.28% when only DLR is enforced. The CR further reduces to 5.14% for OTS. The coordination of OTS and DLR in FTDLR can mitigate network congestion more efficiently

TABLE 3. Generation and loading information for IEEE 24-bus system.

Total Max. First-stage Generators Capacity	2215 MW
Total Max. 2nd-stage Generators Capacity	1160 MW
Load Ramping Requirement (LRR)	345.1 MW
Max. Net load	2950 MW
Min. Net Load	1660 MW

TABLE 4. Congestion results for the IEEE 24-bus system.

Congestion Rate (CR)	SUC	DLR	OTS	FTDLR
	0.0687	0.0628	0.0514	0.0386

by line switching action and increasing the line capacity dynamically. This results in the lowest CR of 3.86%, which improves the system performance by 43.81% in comparison to basic SUC problem.

3) CONTINGENCY ANALYSIS

Contingency analysis (CA) is an essential tool in power system management operations. The objective is to identify those contingencies, which are critical and could affect the reliability of system. The operational performance of the proposed FTDLR model is tested under contingency analysis. In this study, both generator and transmission line contingencies are considered. It should be mentioned that in normal operating conditions all load must be satisfied without any load-shedding. In case of contingencies, load-shedding is allowed, as the primary focus is to study the influence of FTDLR model on system operation cost. There should be sufficient spinning reserves available to counter any contingency, thus, avoiding any load-shedding.

In the first case, the index $\hbar_{g,t,\Omega}$ is iteratively set to zero for all realized scenarios and the cost for each case is noted. For each contingency, $\hbar_{g,t,\Omega}$ is considered zero for all time periods as the time horizon selected is much smaller than the time required for repairing or bringing machine back into operation. The cost of each generator contingency for the four cases is depicted in Figure 6. The values are scaled for better understanding of the results. The costs for SUC is considered as a base case for all the generator contingencies. It can be clearly observed that the incorporation of FTDLR outperforms all other topologies in terms of system operating cost for all generator contingencies except for the case when G3=0. In this case the enforcement of DLR results in less cost savings in comparison to FTDLR. Overall, the joint operation of OTS and DLR proves to save substantial cost savings in case of contingencies.

Congestion rate, wind curtailment, and load-shedding information for each generating unit failure are displayed in Table 5. Potential network congestion exists in basic SUC problem where the CR is the highest among all the test cases. It's obvious that both OTS and DLR when deployed

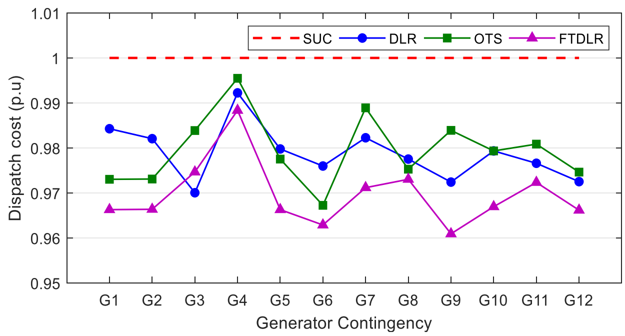

FIGURE 6. Cost information for each generator contingency in IEEE 24-bus System.

TABLE 5. CR, wind curtailment and load-shedding information for generator contingencies.

	Method	G1	G4	G5	G10	G12
Congestion Rate (%)	SUC	6.8	8.5	6.5	6.4	6.5
	DLR	5.7	6.9	5.6	5.8	4.7
	OTS	5.2	6.6	4.8	5.9	6.5
	FTDLR	3.8	6.2	3.2	5.0	4.1
Wind Curtailment (MW)	SUC	2159	1402	2040	2441	1836
	DLR	783.7	235	1205	450.8	437.9
	OTS	1265	524	584.3	251.8	502.2
	FTDLR	169.3	62.7	834	62.29	18.52
Load Shedding (MW)	SUC	0	104	0	0	0.24
	DLR	0	104	0	14.5	0
	OTS	0	104	7.2	0	0
	FTDLR	0	104	2.76	16.5	0

alone still have the capability to relieve system congestion up to some extent. The important manifestation is that the simultaneously deployment of both OTS and DLR can assist relieve network congestion effectively. Due to the inherent flexibility provided by both OTS and DLR, wind power is efficiently consumed with FTDLR. On average 87.99%, 67.03%, and 62.61% more wind power is utilized in FTDLR as opposed to the basic SUC, DLR, and OTS topologies respectively.

Load-shedding is expected to occur in case of contingencies. For most of the generator contingencies, there is no load-shedding in all the test cases except for G4=0 where certain amount of load is curtailed due to insufficient supply. This generator in the network has maximum power generation of 591MW. G4 is located on Bus13 in the network, which is further connected to three other buses i.e. Bus11, Bus12, and Bus23 through transmission lines 18, 20, and 21 respectively. The failure of G4 will be compensated by G11 located on Bus23. But G11 has a maximum capacity of 310MW and it has to serve 5 buses with loads. In this case G11 runs at its maximum power but still unable to cover all the load requirements and ultimately results in Load-shedding. Although the failure of G4 results in the same amount of load-shedding for all test cases, the overall system cost in this scenario is still

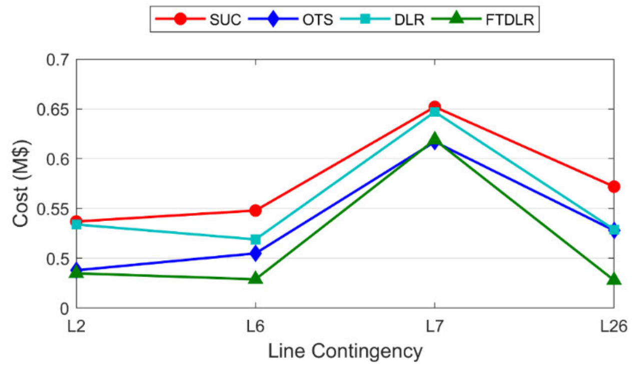

FIGURE 7. Dispatch cost information for line contingency in IEEE 24-bus system.

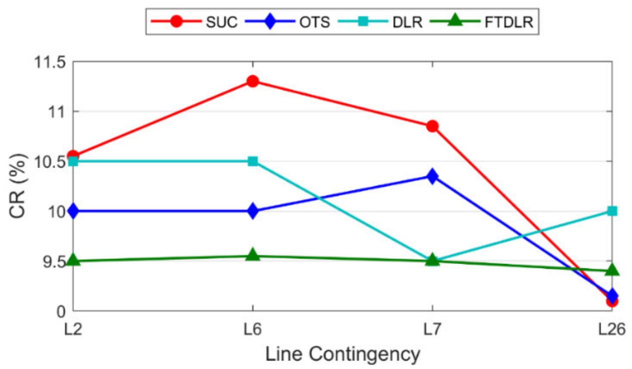

FIGURE 8. Congestion rate information for line contingency in IEEE 24-bus system.

minimum for FTDLR, which is achieved through maximum utilization of wind power generation.

The occurrence of transmission line contingencies in a bulk power system is more often than that of the generator contingencies. Outage of four lines connecting the buses with wind farms are analyzed. These lines contingencies include Line2, Line6, Line7, and Line26. The failure of any of these lines will severely affect the wind power integration as these are the only lines from which wind power can be delivered to other load buses in the system. The results presented in Figure 7 demonstrate that reduction in dispatch cost is highest for FTDLR, followed by OTS, then DLR, and lastly the basic SUC. This reduction in cost is mostly achieved through accommodating more wind power in FTDLR. The CR information given in Figure 8 shows that CR in each contingency is more than 10%, which is why these lines are crucial for safe and secure operation of the network. Wind power is efficiently utilized in FTDLR and wind curtailment is the lowest for FTDLR as compared to all other topologies as shown in Figure 9.

B. IEEE 118-BUS SYSTEM

Although real power networks consists of thousands of buses, their data is not readily available for research, yet to check the feasibility of the FTDLR model it is tested on the larger IEEE 118-bus system besides the IEEE 24-bus system.

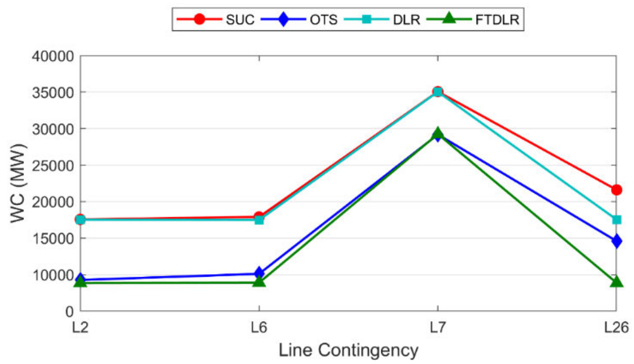

FIGURE 9. Wind curtailment information for line contingency in IEEE 24-bus system.

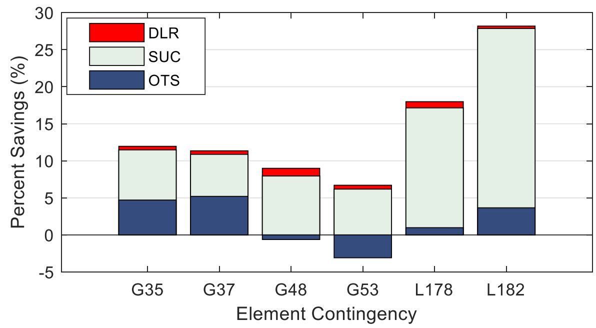

FIGURE 10. System dispatch cost for IEEE 118-bus system contingencies.

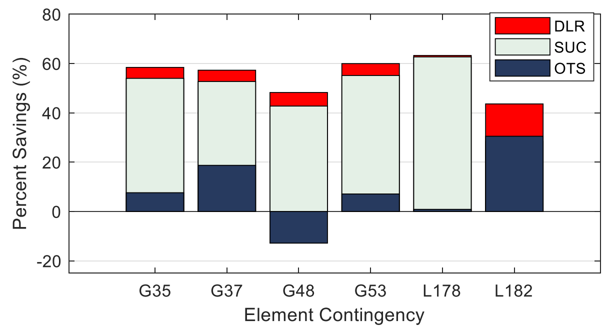

FIGURE 11. Wind power utilization for the IEEE 118-bus system contingencies.

The IEEE 118-bus system includes a total of 118 nodes with 54 generating units and 186 transmission lines. The data for the network is taken from [60]. Some modifications are made to the network to accommodate wind power generation and also induce network congestion. Six wind farms are added to the network at Buses 12, 17, 27, 49, 54, and 80. The total capacity of wind farms is considered to be 1675MW, which comprises 26.9% of the total system peak load. The stopping criteria for the FTDLR model is set as a time limit of 45min and a MIP gap of 0.1%.

Numerical results for the IEEE 118-Bus system are listed in Table 6. System dispatch cost for the base case (SUC) is 1.945M$. The expected cost for OTS and DLR enforced alone are 1.796M$ and 1.696M$ respectively, thereby reducing cost by 7.66% and 12.80% respectively. The incorporation of FTDLR further enhances system performance by reducing dispatch cost to 1.655M$, which is 14.91% less than the base case. The enforcement of FTDLR in the second-stage enables more aggressive decisions for the slow-units in the first-stage decisions.

TABLE 6. Numerical results for the IEEE 118-bus system.

Method	Dispatch Cost (M$)	Cost Savings (%)	Wind Utilization (%)	CR (%)
SUC	1.945	N/A	70.66	9.82
DLR	1.796	7.66	76.6	8.33
OTS	1.696	12.80	82.0	7.94
FTDLR	1.655	14.91	84.17	6.47

Wind power is efficiently utilized in FTDLR allowing the network to dispatch wind power to other load buses in the system; thus helping in system cost reduction. Wind power accommodation capacity can reach up to 84.17% in FTDLR, while in the base case this is about 70.66%. Network congestion mitigation performance of FTDLR in larger network is even more promising. In the base case, 9.82% of lines are congested on average. The CR with OTS and DLR incorporation is 8.33% and 7.94% respectively. System congestion is relieved about 31.11% in FTDLR in comparison to the base case.

When simulating contingency analysis for the IEEE 118-bus system, the most critical elements in the network (both generators and transmission lines), where the highly congested lines can affect system performance, are selected to test the security of the system using the proposed FTDLR model. Only single element contingency is allowed. No multiple or cascaded contingencies are considered in the test cases. The selected contingencies for the test cases are generating units (G35, G37, G48, and G53) and Transmission lines (L178 and L182) respectively.

System dispatch cost, wind power utilization, and CR information for each contingency is shown in Figure 10, Figure 11 and Figure 12 respectively. The results are presented as percent savings in FTDLR as compared to other topologies. The response to each contingency is worst for SUC in terms of system cost, wind power utilization, and network congestion mitigation. The implementation of OTS provides more flexibility to respond to a contingency by changing the network topology. The enforcement of DLR enables power system to increase the power capacity and thus helps in the congestion mitigation during a contingency. For the six contingencies tested, the cost savings for FTDLR can reach up to 28.18%, 27.85%, and 5.20% as compared to SUC, DLR, and OTS respectively. For G48 and G53 contingencies, OTS alone performs better than FTDLR,

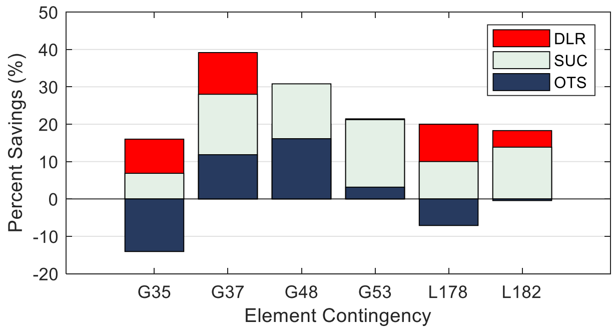

FIGURE 12. Congestion management performance for the IEEE 118-bus system contingencies.

which reduces system cost by 0.68% and 3.02% respectively. Due to the combined flexibility provided by OTS and DLR, FTDLR accommodates more wind power in each contingency except for the G48 contingency where OTS alone accommodates more wind power (12.83%) as compared to FTDLR. The wind power utilization for FTDLR in these contingencies can reach up to 63.24%. Potential network congestion can be mitigated by up to 39.16% in FTDLR as compared to SUC. This demonstrates that the FTDLR model can also improve or maintain system reliability even in case of contingencies.

IV. CONCLUSION

With the increasing wind power integration, power system needs regular investment in transmission infrastructure to cope with increasing load demand and network congestion. In this context, a co-optimized model is presented to investigate the flexibility offered by the transmission system using OTS in coordination with DLR. System assets in combination with RES to enhance the proficiency of the network with the current infrastructure are explored. The optimization model is used to identify candidate lines to be taken off service from the network and increase the current carrying capability of overhead transmission lines based on the predicted weather conditions. The optimization problem can help boost the utilization efficiency of the network, which can help defer the need for building new infrastructure. Performing a comprehensive analysis on IEEE 24-bus and IEEE 118-bus networks, the effect of the coordinated operation is quantified on system cost, network congestion management, and wind power utilization in base case as well as considering network element contingencies. Numerical test results conducted on IEEE 24-bus system validated that with FTDLR, the service operator could substantially reduce system dispatch cost by 22.28%, improve wind power utilization up to 96.84%, and relieve network congestion 43.81% in the normal operating conditions. The operational performance of the proposed FTDLR model is further tested under contingency analysis. It is observed that the incorporation of FTDLR outperforms all other topologies in terms of system operating cost, wind power utilization, and congestion mitigation for all the tested contingencies. The fitness and scalability of the FTDLR model is also investigated on a larger network of the IEEE 118-bus system. The results performed on IEEE 118-Bus system are consistent with that of the IEEE 24-bus system.

The proposed co-optimized model can be utilized to take maximum advantage of the wind power integration while at the same time postponing the need for upgrading or constructing new transmission infrastructure. It can be concluded that the deployment of the proposed optimization model can add to the effective utilization of the renewable generation. The model can be extended in future to include more robust algorithms for solving the problem, impact on power system reliability, and testing the model with AC settings.

REFERENCES

[1] H. Quan, D. Srinivasan, A. M. Khambadkone, and A. Khosravi, "A computational framework for uncertainty integration in stochastic unit commitment with intermittent renewable energy sources," *Appl. Energy*, vol. 152, pp. 71–82, Aug. 2015, doi: 10.1016/j.apenergy.2015.04.103.

[2] H. Schermeyer, C. Vergara, and W. Fichtner, "Renewable energy curtailment: A case study on today's and tomorrow's congestion management," *Energy Policy*, vol. 112, pp. 427–436, Jan. 2018.

[3] P. Eser, A. Singh, N. Chokani, and R. S. Abhari, "Effect of increased renewables generation on operation of thermal power plants," *Appl. Energy*, vol. 164, pp. 723–732, Feb. 2016, doi: 10.1016/j.apenergy.2015.12.017.

[4] E. B. Fisher, R. P. O'Neill, and M. C. Ferris, "Optimal transmission switching," *IEEE Trans. Power Syst.*, vol. 23, no. 3, pp. 1346–1355, Aug. 2008, doi: 10.1109/TPWRS.2008.922256.

[5] K. W. Hedman, S. S. Oren, and R. P. O'Neill, "Optimal transmission switching: Economic efficiency and market implications," *J. Regulatory Econ.*, vol. 40, no. 2, pp. 111–140, Oct. 2011, doi: 10.1007/s11149-011-9158-z.

[6] M. Peker, A. S. Kocaman, and B. Y. Kara, "Benefits of transmission switching and energy storage in power systems with high renewable energy penetration," *Appl. Energy*, vol. 228, pp. 1182–1197, Oct. 2018, doi: 10.1016/j.apenergy.2018.07.008.

[7] J. Han and A. Papavasiliou, "The impacts of transmission topology control on the European electricity network," *IEEE Trans. Power Syst.*, vol. 31, no. 1, pp. 496–507, Jan. 2016, doi: 10.1109/TPWRS.2015.2408439.

[8] W. Shao and V. Vittal, "New algorithm for relieving overloads and voltage violations by transmission line and bus-bar switching," in *Proc. IEEE PES Power Syst. Conf. Expo.*, Oct. 2004, pp. 322–327, doi: 10.1109/PSCE.2004.1397509.

[9] A. Nikoobakht, J. Aghaei, M. Mardaneh, T. Niknam, and V. Vahidinasab, "Moving beyond the optimal transmission switching: Stochastic linearised SCUC for the integration of wind power generation and equipment failures uncertainties," *IET Gener., Transmiss. Distrib.*, vol. 12, no. 15, pp. 3780–3792, Aug. 2018, doi: 10.1049/iet-gtd.2017.0617.

[10] F. Qiu and J. Wang, "Chance-constrained transmission switching with guaranteed wind power utilization," *IEEE Trans. Power Syst.*, vol. 30, no. 3, pp. 1270–1278, May 2015, doi: 10.1109/TPWRS.2014.2346987.

[11] A. Nikoobakht, J. Aghaei, and M. Mardaneh, "Securing highly penetrated wind energy systems using linearized transmission switching mechanism," *Appl. Energy*, vol. 190, pp. 1207–1220, Mar. 2017, doi: 10.1016/j.apenergy.2016.12.146.

[12] M. Numan, D. Feng, F. Abbas, S. Habib, and A. Rasool, "Mobilizing grid flexibility through optimal transmission switching for power systems with large-scale renewable integration," *Int. Trans. Electr. Energy Syst.*, vol. 30, no. 3, pp. 1–15, Mar. 2020, doi: 10.1002/2050-7038.12211.

[13] J. Shi and S. S. Oren, "Stochastic unit commitment with topology control recourse for power systems with large-scale renewable integration," *IEEE Trans. Power Syst.*, vol. 33, no. 3, pp. 3315–3324, May 2018, doi: 10.1109/TPWRS.2017.2772168.

[14] E. Little, S. Bortolotti, J. Bourmaud, E. Karangelos, and Y. Perez, "Optimal transmission topology for facilitating the growth of renewable power generation," 2021, *arXiv:2103.15677*. [Online]. Available: https://arxiv.org/abs/2103.15677

[15] A. R. Escobedo, E. Moreno-Centeno, and K. W. Hedman, "Topology control for load shed recovery," *IEEE Trans. Power Syst.*, vol. 29, no. 2, pp. 908–916, Mar. 2014, doi: 10.1109/TPWRS.2013.2286009.

[16] J. C. Villumsen, G. Bronmo, and A. B. Philpott, "Line capacity expansion and transmission switching in power systems with large-scale wind power," *IEEE Trans. Power Syst.*, vol. 28, no. 2, pp. 731–739, May 2013, doi: 10.1109/TPWRS.2012.2224143.

[17] A. Khodaei, M. Shahidehpour, and S. Kamalinia, "Transmission switching in expansion planning," *IEEE Trans. Power Syst.*, vol. 25, no. 3, pp. 1722–1733, Aug. 2010, doi: 10.1109/TPWRS.2009.2039946.

[18] K. W. Hedman, M. C. Ferris, R. P. O'Neill, E. B. Fisher, and S. S. Oren, "Co-optimization of generation unit commitment and transmission switching with N-1 reliability," *IEEE Trans. Power Syst.*, vol. 25, no. 2, pp. 1052–1063, May 2010, doi: 10.1109/TPWRS.2009.2037232.

[19] P. M. de Quevedo, J. Contreras, M. J. Rider, and J. Allahdadian, "Contingency assessment and network reconfiguration in distribution grids including wind power and energy storage," *IEEE Trans. Sustain. Energy*, vol. 6, no. 4, pp. 1524–1533, Oct. 2015, doi: 10.1109/TSTE.2015.2453368.

[20] M. Li, P. B. Luh, L. D. Michel, Q. Zhao, and X. Luo, "Corrective line switching with security constraints for the base and contingency cases," *IEEE Trans. Power Syst.*, vol. 27, no. 1, pp. 125–133, Feb. 2012, doi: 10.1109/TPWRS.2011.2164098.

[21] M. Abdi-Khorsand, M. Sahraei-Ardakani, and Y. M. Al-Abdullah, "Corrective transmission switching for N-1-1 contingency analysis," *IEEE Trans. Power Syst.*, vol. 32, no. 2, pp. 1606–1615, Mar. 2016, doi: 10.1109/TPWRS.2016.2614520.

[22] A. Khodaei and M. Shahidehpour, "Security-constrained transmission switching with voltage constraints," *Int. J. Electr. Power Energy Syst.*, vol. 35, no. 1, pp. 74–82, Feb. 2012, doi: 10.1016/j.ijepes.2011.09.014.

[23] A. Khodaei and M. Shahidehpour, "Transmission switching in security-constrained unit commitment," *IEEE Trans. Power Syst.*, vol. 25, no. 4, pp. 1937–1945, Nov. 2010, doi: 10.1109/TPWRS.2010.2046344.

[24] G. Granelli, M. Montagna, F. Zanellini, P. Bresesti, R. Vailati, and M. Innorta, "Optimal network reconfiguration for congestion management by deterministic and genetic algorithms," *Electr. Power Syst. Res.*, vol. 76, nos. 6–7, pp. 549–556, Apr. 2006, doi: 10.1016/j.epsr.2005.09.014.

[25] S. R. Salkuti, "Congestion management using optimal transmission switching," *IEEE Syst. J.*, vol. 12, no. 4, pp. 3555–3564, Dec. 2018, doi: 10.1109/JSYST.2018.2808260.

[26] S. Dehghan, N. Amjady, and S. Member, "Robust transmission and energy storage expansion planning in wind farm-integrated power systems considering transmission switching," *IEEE Trans. Sustain. Energy* vol. 7, no. 2, pp. 1–10, Dec. 2015.

[27] R. A. Jabr, I. Dzafic, and B. C. Pal, "Robust optimization of storage investment on transmission networks," *IEEE Trans. Power Syst.*, vol. 30, no. 1, pp. 531–539, Jan. 2015.

[28] A. V. Ramesh and X. Li, "Network reconfiguration impact on renewable energy system and energy storage system in day-ahead scheduling," 2021, *arXiv:2103.13321*. [Online]. Available: https://arxiv.org/abs/2103.13321

[29] Y. Bai, H. Zhong, Q. Xia, and C. Kang, "A two-level approach to AC optimal transmission switching with an accelerating technique," *IEEE Trans. Power Syst.*, vol. 32, no. 2, pp. 1616–1625, Jun. 2016, doi: 10.1109/TPWRS.2016.2582214.

[30] A. Papavasiliou, S. S. Oren, and B. Rountree, "Applying high performance computing to transmission-constrained stochastic unit commitment for renewable energy integration," *IEEE Trans. Power Syst.*, vol. 30, no. 3, pp. 1109–1120, May 2015, doi: 10.1109/TPWRS.2014.2341354.

[31] C. Liu, J. Wang, and J. Ostrowski, "Heuristic prescreening switchable branches in optimal transmission switching," *IEEE Trans. Power Syst.*, vol. 27, no. 4, pp. 2289–2290, Nov. 2012, doi: 10.1109/TPWRS.2012.2193489.

[32] A. Papavasiliou, S. S. Oren, Z. Yang, P. Balasubramanian, and K. Hedman, "An application of high performance computing to transmission switching," in *Proc. IREP Symp. Bulk Power Syst. Dyn. Control 9th Optim., Secur. Control Emerg. Power Grid*, Aug. 2013, pp. 1–6, doi: 10.1109/IREP.2013.6629392.

[33] P. Balasubramanian, M. Sahraei-Ardakani, X. Li, and K. W. Hedman, "Towards smart corrective switching: Analysis and advancement of PJM's switching solutions," *IET Gener., Transmiss. Distrib.*, vol. 10, no. 8, pp. 1984–1992, May 2016, doi: 10.1049/iet-gtd.2015.1362.

[34] M. Sahraei-Ardakani, X. Li, P. Balasubramanian, K. W. Hedman, and M. Abdi-Khorsand, "Real-time contingency analysis with transmission switching on real power system data," *IEEE Trans. Power Syst.*, vol. 31, no. 3, pp. 2501–2502, May 2016, doi: 10.1109/TPWRS.2015.2465140.

[35] B. P. Bhattarai, J. P. Gentle, T. McJunkin, P. J. Hill, K. S. Myers, A. W. Abboud, R. Renwick, and D. Hengst, "Improvement of transmission line ampacity utilization by weather-based dynamic line rating," *IEEE Trans. Power Del.*, vol. 33, no. 4, pp. 1853–1863, Aug. 2018, doi: 10.1109/TPWRD.2018.2798411.

[36] N. Doban, "Building predictive models for dynamic line rating using data science techniques," M.S. thesis, School Archit. Community Building, KTH Roy. Inst. Technol., Stockholm, Sweden, 2016.

[37] A. Michiorri, H.-M. Nguyen, S. Alessandrini, J. B. Bremnes, S. Dierer, E. Ferrero, B.-E. Nygaard, P. Pinson, N. Thomaidis, and S. Uski, "Forecasting for dynamic line rating," *Renew. Sustain. Energy Rev.*, vol. 52, pp. 1713–1730, Dec. 2015, doi: 10.1016/j.rser.2015.07.134.

[38] F. Qiu and J. Wang, "Distributionally robust congestion management with dynamic line ratings," *IEEE Trans. Power Syst.*, vol. 30, no. 4, pp. 2198–2199, Jul. 2015, doi: 10.1109/TPWRS.2014.2361012.

[39] J. Zhan, W. Liu, and C. Y. Chung, "Stochastic transmission expansion planning considering uncertain dynamic thermal rating of overhead lines," *IEEE Trans. Power Syst.*, vol. 34, no. 1, pp. 432–443, Jan. 2019, doi: 10.1109/TPWRS.2018.2857698.

[40] M. Nick, O. Alizadeh-Mousavi, R. Cherkaoui, and M. Paolone, "Security constrained unit commitment with dynamic thermal line rating," *IEEE Trans. Power Syst.*, vol. 31, no. 3, pp. 2014–2025, May 2016.

[41] H. Park, Y. G. Jin, and J.-K. Park, "Stochastic security-constrained unit commitment with wind power generation based on dynamic line rating," *Int. J. Electr. Power Energy Syst.*, vol. 102, pp. 211–222, Nov. 2018, doi: 10.1016/j.ijepes.2018.04.026.

[42] J. Shi and S. S. Oren, "Flexible line ratings in stochastic unit commitment for power systems with large-scale renewable generation," *Energy Syst.*, vol. 11, no. 1, pp. 1–19, Feb. 2020, doi: 10.1007/s12667-018-0306-8.

[43] E. Fernandez, I. Albizu, M. T. Bedialauneta, A. J. Mazon, and P. T. Leite, "Review of dynamic line rating systems for wind power integration," *Renew. Sustain. Energy Rev.*, vol. 53, pp. 80–92, Jan. 2016, doi: 10.1016/j.rser.2015.07.149.

[44] T. O. Seppa, "Increasing transmission capacity by real time monitoring," in *Proc. IEEE Power Eng. Soc. Winter Meeting. Conf.*, Jan. 2003, pp. 1208–1211, doi: 10.1109/PESW.2002.985201.

[45] D. M. Kim and J. O. Kim, "Prediction of transmission-line rating based on thermal overload probability using weather models," *Eur. Trans. Elect. Power*, vol. 20, no. 4, pp. 534–544, 2010, doi: 10.1002/etep.

[46] Y. Li, B. Hu, K. Xie, L. Wang, Y. Xiang, R. Xiao, and D. Kong, "Day-ahead scheduling of power system incorporating network topology optimization and dynamic thermal rating," *IEEE Access*, vol. 7, pp. 35287–35301, 2019, doi: 10.1109/ACCESS.2019.2904877.

[47] Y. Li, K. Xie, R. Xiao, B. Hu, H. Chao, and D. Kong, "Network-constrained unit commitment incorporating dynamic thermal rating and transmission line switching," in *Proc. 2nd IEEE Conf. Energy Internet Energy Syst. Integr. (EI)*, Oct. 2018, pp. 1–6, doi: 10.1109/EI2.2018.8582182.

[48] R. Xiao, Y. Xiang, L. Wang, and K. Xie, "Power system reliability evaluation incorporating dynamic thermal rating and network topology optimization," *IEEE Trans. Power Syst.*, vol. 33, no. 6, pp. 6000–6012, Nov. 2018, doi: 10.1109/TPWRS.2018.2829079.

[49] M. Jabarnejad and J. Valenzuela, "Optimal investment plan for dynamic thermal rating using benders decomposition," *Eur. J. Oper. Res.*, vol. 248, no. 3, pp. 917–929, Feb. 2016, doi: 10.1016/j.ejor.2015.08.010.

[50] M. Numan, D. Feng, F. Abbas, U. Rahman, and W. A. Wattoo, "Impact assessment of a co-optimized dynamic line rating and transmission switching topology on network expansion planning," *Int. Trans. Electr. Energy Syst.*, vol. 30, no. 8, pp. 1–24, Aug. 2020, doi: 10.1002/2050-7038.12457.

[51] P. A. Ruiz, C. R. Philbrick, and P. W. Sauer, "Wind power day-ahead uncertainty management through stochastic unit commitment policies," in *Proc. IEEE/PES Power Syst. Conf. Expo.*, Mar. 2009, pp. 1–9, doi: 10.1109/PSCE.2009.4840133.

[52] *Guide for Thermal Rating of Overhead Lines*, Standard 601. 2014, CIGRE Technical Brochure, 2014.

[53] *IEEE Standard for Calculating the Current-Temperature Relationship of Bare Overhead Conductors*, IEEE Power Engineering Society, IEEE Standard 738, 2007.

[54] *Overhead Electrical Conductors—Calculation Methods for Stranded Bare Conductors*, Standard IEC/TR 61597 1995, 1995.

[55] J. Shi and S. S. Oren, "Wind power integration through stochastic unit commitment with topology control recourse," in *Proc. Power Syst. Comput. Conf. (PSCC)*, Jun. 2016, pp. 1–7, doi: 10.1109/PSCC.2016.7541026.

[56] M. Numan, D. Feng, F. Abbas, S. Habib, and S. Hao, "Coordinated operation of reconfigurable networks with dynamic line rating for optimal utilization of renewable generation," *Int. J. Electr. Power Energy Syst.*, vol. 125, Feb. 2021, Art. no. 106473, doi: 10.1016/j.ijepes.2020.106473.

[57] C. Grigg, P. Wong, P. Albrecht, R. Allan, M. Bhavaraju, R. Billinton, Q. Chen, C. Fong, S. Haddad, S. Kuruganty, W. Li, R. Mukerji, D. Patton, N. Rau, D. Reppen, A. Schneider, M. Shahidehpour, and C. Singh, "The IEEE reliability test system-1996. A report prepared by the reliability test system task force of the application of probability methods subcommittee," *IEEE Trans. Power Syst.*, vol. 14, no. 3, pp. 1010–1020, Aug. 1999, doi: 10.1109/59.780914.

[58] A. Papavasiliou and S. S. Oren, "Multiarea stochastic unit commitment for high wind penetration in a transmission constrained network," *Oper. Res.*, vol. 61, no. 3, pp. 578–592, Jun. 2013, doi: 10.1287/opre.2013.1174.

[59] N. Growe-Kuska, H. Heitsch, and W. Romisch, "Scenario reduction and scenario tree construction for power management problems," in *Proc. IEEE Bologna Power Tech Conf.*, Jun. 2003, p. 7, doi: 10.1109/PTC.2003.1304379.

[60] *University of Washington Power System Test Case Archive n.d.* Accessed: Mar. 2020. [Online]. Available: https://labs.ece.uw.edu/pstca/

MUHAMMAD NUMAN received the B.Eng. degree in electrical engineering from the National University of Sciences and Technology (NUST), Karachi, Pakistan, in 2013, the M.Sc. degree in electric power system from North China Electric Power University (NCEPU), Beijing, China, in 2016, and the Ph.D. degree in electrical engineering from Shanghai Jiao Tong University (SJTU), Shanghai, China, in 2021. He is currently serving as an Assistant Professor for the U.S.-Pakistan Centers for Advanced Studies in Energy, NUST, Islamabad, Pakistan. His current research interests include power system optimization, network expansion planning, transmission network topologies, and renewable energy.

AKIF ZIA KHAN received the B.Eng. degree in electrical engineering from the National University of Sciences and Technology (NUST), Islamabad, Pakistan, in 2011, the M.Sc. degree in electric power systems from North China Electric Power University, Beijing, China, in 2014, and the Ph.D. degree in power electronics from The Hong Kong Polytechnic University, Hong Kong, SAR, China, in 2020. From 2014 to 2016, he has served as a Lecturer for the U.S.-Pakistan Center for Advanced Studies in Energy, NUST. During the spring of 2016, he was a Visiting Research Scholar with the Power Systems Engineering Research Center, Arizona State University, Tempe, AZ, USA. In 2019, he was a Visiting Ph.D. Scholar with the Center of Reliable Power Electronics, Department of Energy Technology, Aalborg University, Denmark. He is currently serving as an Assistant Professor for the U.S.-Pakistan Center for Advanced Studies in Energy, NUST. He contributes regularly as a reviewer of various international journals and conferences. His current research interests include design, modeling, and control of high-power and high-frequency bidirectional resonant power converters for various power processing applications.

MANSOOR ASIF was born in Pakistan, in 1991. He received the bachelor's degree in electrical engineering from the National University of Sciences and Technology (NUST), Pakistan, in 2013, the master's degree in electric power systems from North China Electric Power University, Beijing, in 2015, and the Ph.D. degree in electrical engineering from Hanyang University, South Korea, in 2020. He is currently working as an Assistant Professor with the School of Electrical Engineering and Computer Science, NUST. His current research interests include overvoltage analysis, and insulation coordination and analysis of different transient phenomenon in power systems.

SARMAD MAJEED MALIK received the B.S. degree in electronics engineering from the National University of Sciences and Technology (NUST), Pakistan, and the M.S. and Ph.D. degrees in electrical engineering from North China Electric Power University (NCEPU), China. He is currently serving as an Assistant Professor for the Department of Electrical Engineering, NUST. His research interests include microgrids, renewable energy, and control of converters applications.

KASHIF IMRAN received the B.Sc. and M.Sc. degrees in electrical engineering from the University of Engineering and Technology (UET) Lahore, in 2006 and 2008, respectively. He secured a Commonwealth Scholarship and received the Ph.D. degree in electrical engineering from the University of Strathclyde, in 2015. He worked with the Transmission and Distribution Division of SIEMENS and the Power Distribution Design Section of NESPAK, from 2006 to 2007. He has worked as a Faculty Member with the University of Engineering and Technology (UET) Lahore and COMSATS University Islamabad. He is currently an Associate Professor and the inaugural Head of the Department of Electrical Power Engineering, U.S.-Pakistan Center for Advanced Studies in Energy, National University of Sciences and Technology, Islamabad. His research interests include applications of artificial intelligence and computational techniques to the planning and operations of power systems and electricity markets.